

On the resolution of cosmic coincidence problem and phantom crossing with triple interacting fluids

Mubasher Jamil*, Farook Rahaman†

*Center for Advanced Mathematics and Physics, National University of Sciences and Technology,
Peshawar Road, Rawalpindi - 46000, Pakistan

†Department of Mathematics, Jadavpur University, Kolkata - 700032, India

September 3, 2019

Abstract

We here investigate a cosmological model in which three fluids interact with each other involving certain coupling parameters and energy exchange rates. The motivation of the problem stems from the puzzling ‘triple coincidence problem’ which naively asks why the cosmic energy densities of matter, radiation and dark energy are almost of the same order of magnitude at the present time. In our model, we determine the conditions under triple interacting fluids will cross the phantom divide.

Keywords: Interacting dark energy; cosmological constant; cosmic coincidence problem; phantom energy; phantom crossing.

*mjamil@camp.edu.pk

†farook_rahaman@yahoo.com

1 Introduction

Despite several successes of the standard big bang cosmology based on Friedmann-Robertson-Walker (FRW) model, still a series of problems to be resolved like the horizon problem, flatness problem, dark matter (or missing mass) problem, structure formation, topological defects, matter-antimatter asymmetry and the cosmic coincidence problem etc. Most of these are related with the cosmic past of the observable universe while the cosmic coincidence problem has its origin in the recent time since it naively asks why certain cosmological phenomena are occurring in our presence or in our times. Recent astrophysical observations give convincing evidence of an accelerating universe caused by dark energy characterized by the equation of state (EoS) parameter $\omega \simeq -1$. It is yet unknown why the present energy density of the dark energy is approximately equal to that of dust-like matter. It is termed as the cosmic coincidence problem [1]. Till now several models have been proposed in an attempt to solve this problem such as the ‘tracker field’ [2], oscillating dark energy [3] and the variable constants approach [4], to name a few. It appears that the energy density of the radiation component is also almost equivalent to that of the matter and the dark energy i.e. $\rho_m \sim \rho_r \sim \rho_\Lambda$ or $\Omega_m \sim \Omega_r \sim \Omega_\Lambda$, the so-called ‘cosmic triple coincidence problem’ [5]. The question is: why this happens in the current or in recent times. The history of the parameter ω suggests that it is no more a constant but possesses a parametric form $\omega(z)$, where z is the redshift parameter. Thus in the past $\omega = 1/3$ corresponds to radiation and then $\omega = 0$ for matter. Later it evolved to quintessence $\omega < -1/3$ to cosmological constant $\omega = -1$. This behavior suggests that in future, ω will be super-negative i.e. $\omega < -1$, which corresponds to the phantom energy. Thus in totality, we have the transition from $\omega > -1$ to $\omega < -1$ the so-called ‘phantom crossing’ or ‘phantom divide’ scenario, while we are observing $\omega = -1$ at the current time [6]. The coincidence problem in this context is rephrased as ‘why is $\omega = -1$ now?’

In recent years, the usual coincidence problem is addressed by proposing an exotic interaction between dark energy and matter in which energy from ρ_Λ is diluted or decayed into the ρ_m [7, 8, 9, 10, 11, 12, 13, 14, 15, 16, 17, 18]. It is recently proposed that if these two components interact then some energy might dissipate into a third component ρ_x which is as yet hypothetical [19]. The third component can be known form of matter or an altogether exotic fluid in which case some new physics will be required to explain the interaction. If we assume $\rho_x = \rho_r$ then the interaction between three fluids i.e. matter, radiation and dark energy will be quite interesting. It is well-known that matter and radiation were decoupled at the time of emission of cosmic microwave background (CMB) radiation at a redshift $z \sim 1100$. Thus both matter and radiation are almost non-interacting components but it can be anticipated that these two components do supposedly interact with the dark energy. Thus if dark energy and matter interact, the energy dissipated in the interaction is assumed to transfer to the radiation component and vice

versa for the radiation and the dark energy interaction. This dynamic interaction than hugely alters the effective equation of state of the three interacting fluids. Our analysis in this paper suggests that effective EoS of the three fluids will be interlinked to each other considerably and also constrained by coupling parameters. Moreover, the interaction naturally leads to the phantom crossing scenario.

We here present a model in which three cosmic fluids (radiation, matter and dark energy) interact with each other with equal degree of freedom. Hence there are three coupling parameters involved which can take arbitrary positive or negative values not all zero simultaneously. The positive and negative values correspond to back and forth nature of energy exchange between the fluids. We emphasis here that the coupling parameters in our model are only constrained by the choices of effective EoS of the fluids. Thus in our model, exact EoS of the fluids like in the non-interacting FRW model is not possible. As the exact EoS for the dark energy is unknown, its interaction with other fluids creates ambiguities in the determination of the exact EoS of the other fluids. Hence we also stress that precise values of the EoS's can be deduced only empirically from the phenomenology of the interacting fluids.

2 The model of triple interacting fluids

We start by assuming the background to be spatially flat, homogeneous and isotropic FRW spacetime

$$ds^2 = -dt^2 + a^2(t) \left[dr^2 + r^2(d\theta^2 + \sin^2\theta d\phi^2) \right], \quad (1)$$

where $a(t)$ is the scale factor. We consider three fluids having the equations of state (EoS) $p_i = \omega_i \rho_i$, $i = 1, 2, 3$ where p_i and ρ_i are the corresponding pressures and the energy densities of the fluids, respectively. Also ω_i are the dimensionless EoS parameters. For the sake of simplicity, we assume the three fluids to be perfect fluid-like since in general, interaction between fluids might lead to local inhomogeneities, which are ignored in the present paper. The equations governing the interaction of three fluids are expressed as

$$\dot{\rho}_1 + 3H(1 + \omega_1)\rho_1 = Q_3 - Q_2, \quad (2)$$

$$\dot{\rho}_2 + 3H(1 + \omega_2)\rho_2 = Q_1 - Q_3, \quad (3)$$

$$\dot{\rho}_3 + 3H(1 + \omega_3)\rho_3 = Q_2 - Q_1. \quad (4)$$

Here Q_i are the energy exchange (or dissipative) terms to be put ad hoc in the above equations. The explicit form of Q_i should be determined only from the phenomenological and empirical results. However, from dimensional considerations, the quantity Q_i should have dimensions of density into the time inverse. Choosing the later one to be Hubble parameter, we notice that Q_i can be of the following forms: $Q_i \simeq H\rho_i$. This approximation

can be saturated to equality by inserting a dimensionless parameter (say λ_i). Thus we can write [20] (see [21] for more exotic expressions for Q_i)

$$Q_i = \lambda_i H \rho_{io} a^{-3(1+\omega_i)}, \quad i = 1, 2, 3. \quad (5)$$

In the last expression, λ_i are the coupling constants which can take positive or negative values to yield two-sided energy exchange rather than one-sided. Also Eqs. (2) to (5) show that this a coupled system of three differential equations which needs to be solved. Further ρ_{io} are the constant energy densities at some reference time $t = t_o$. Also $H \equiv \dot{a}/a$ is Hubble parameter which determines the rate of expansion of the universe. Sum of Eqs. (2) to (4) yield the combined energy conservation

$$\sum_{i=1}^3 [\dot{\rho}_i + 3H(1 + \omega_i)\rho_i] = 0, \quad (6)$$

Also the energy conservation for the individual component (for the case of non-interacting fluids) yields

$$\rho'_i = \rho_{io} a^{-3(1+\omega_i)}, \quad i = 1, 2, 3. \quad (7)$$

Here ρ_{io} are integration constants. Combining Eqs. (2), (3) and (4), we arrive at the density evolution of the interacting fluids as

$$\rho_1 = C_1 a^{-3(1+\omega_1)} + \frac{\lambda_2 \rho_{2o}}{3} \frac{a^{-3(1+\omega_2)}}{\omega_2 - \omega_1} + \frac{\lambda_3 \rho_{3o}}{3} \frac{a^{-3(1+\omega_3)}}{\omega_1 - \omega_3}, \quad (8)$$

$$\rho_2 = C_2 a^{-3(1+\omega_2)} + \frac{\lambda_3 \rho_{3o}}{3} \frac{a^{-3(1+\omega_3)}}{\omega_3 - \omega_2} + \frac{\lambda_1 \rho_{1o}}{3} \frac{a^{-3(1+\omega_1)}}{\omega_2 - \omega_1}, \quad (9)$$

$$\rho_3 = C_3 a^{-3(1+\omega_3)} + \frac{\lambda_1 \rho_{1o}}{3} \frac{a^{-3(1+\omega_1)}}{\omega_1 - \omega_3} + \frac{\lambda_2 \rho_{2o}}{3} \frac{a^{-3(1+\omega_2)}}{\omega_3 - \omega_2}. \quad (10)$$

Here C_i 's are constants of integration. Now addition of Eqs. (8), (9) and (10) results in

$$\rho = \rho'_1 X_1 + \rho'_2 X_2 + \rho'_3 X_3, \quad (11)$$

where

$$X_1 = 1 + \frac{\lambda_1}{3} \frac{\omega_2 - \omega_3}{(\omega_1 - \omega_3)(\omega_2 - \omega_1)}, \quad (12)$$

$$X_2 = 1 + \frac{\lambda_2}{3} \frac{\omega_3 - \omega_1}{(\omega_2 - \omega_1)(\omega_3 - \omega_2)}, \quad (13)$$

$$X_3 = 1 + \frac{\lambda_3}{3} \frac{\omega_1 - \omega_2}{(\omega_1 - \omega_3)(\omega_3 - \omega_2)}. \quad (14)$$

Here we have assumed $C_i = \rho_{io}$ and $\rho \equiv \rho_1 + \rho_2 + \rho_3$ is the total energy density of the interacting fluids. Note that the case of non-interacting fluids is obtained by choosing

$\lambda_1 = \lambda_2 = \lambda_3 = 0$ which yield $X_1 = X_2 = X_3 = 1$ i.e. $\rho = \rho'_1 + \rho'_2 + \rho'_3$. Using the first FRW equation

$$H^2 = \frac{8\pi G}{3}\rho. \quad (15)$$

Differentiating Eq. (7) w.r.t t , we obtain

$$\dot{\rho}'_i = -3(1 + \omega_i)H\rho_{i0}a^{-3(1+\omega_i)}, \quad i = 1, 2, 3. \quad (16)$$

Differentiating Eq. (15) w.r.t t and then using Eqs. (11) and (16), we find

$$\dot{H} = -H\sqrt{24\pi G}\sum_{i=1}^3[\rho'_i(1 + \omega_i)X_i]\left(\sum_{i=1}^3\rho'_iX_i\right)^{-1/2}. \quad (17)$$

2.1 Role of parameter \dot{H}

The parameter \dot{H} is significant as its possible signature governs the dynamics of the universe [25]. For instance $\dot{H} < 0$ represents the deceleration phase of the expanding universe. This slowing down in the expansion takes place when

$$\omega_1 > -1, \quad \lambda_1 > \frac{3(\omega_1 - \omega_3)(\omega_2 - \omega_1)}{\omega_3 - \omega_2}, \quad (18)$$

$$\omega_2 > -1, \quad \lambda_2 > \frac{3(\omega_2 - \omega_1)(\omega_3 - \omega_2)}{\omega_1 - \omega_3}, \quad (19)$$

$$\omega_3 > -1, \quad \lambda_3 > \frac{3(\omega_1 - \omega_3)(\omega_3 - \omega_2)}{\omega_2 - \omega_1}. \quad (20)$$

Thus \dot{H} will be negative when all the $\omega_i > -1$. This result corresponds to the quintessence dominated universe.

Note that the vanishing \dot{H} in Eq. (17) will yield a de Sitter universe or a cosmological constant dominated universe i.e.

$$\dot{H} = 0 \implies \omega_1 = \omega_2 = \omega_3 = -1. \quad (21)$$

Moreover $\dot{H} > 0$ corresponds to an accelerating universe. This situation arises in our model when

$$(1 + \omega_1)X_1 < 0, \quad (22)$$

$$(1 + \omega_2)X_2 < 0, \quad (23)$$

$$(1 + \omega_3)X_3 < 0. \quad (24)$$

The above Eqs. (22), (23) and (24) yield respectively

$$\omega_1 < -1, \quad \lambda_1 > \frac{3(\omega_1 - \omega_3)(\omega_2 - \omega_1)}{\omega_3 - \omega_2}, \quad (25)$$

$$\omega_2 < -1, \quad \lambda_2 > \frac{3(\omega_2 - \omega_1)(\omega_3 - \omega_2)}{\omega_1 - \omega_3}, \quad (26)$$

$$\omega_3 < -1, \quad \lambda_3 > \frac{3(\omega_1 - \omega_3)(\omega_3 - \omega_2)}{\omega_2 - \omega_1}. \quad (27)$$

Thus \dot{H} will be positive when all the $\omega_i < -1$. This result corresponds to the phantom energy dominated universe. Note that the coupling parameters λ_i have to be positive both for the decelerating and the accelerating universe. This result turns out to be consistent with [22] that coupling parameters cannot be negative to avoid violation of second law of thermodynamics. Moreover the same investigation shows that small positive values for the coupling parameters are motivated from the empirical results. Therefore the universe evolves from the earlier quintessence to cosmological constant and then later to the phantom energy dominated universe.

2.2 Behavior of deceleration parameter

The deceleration parameter $q \sim \dot{H} + H^2 = -8\pi G \sum_{i=1}^3 [\rho'_i(\frac{2}{3} + \omega_i)X_i]$. The parameter q is significant as its possible signature governs the dynamics of the universe. For instance $q < 0$ represents the acceleration phase of the expanding universe. This slowing down in the expansion takes place when

$$\omega_1 > -\frac{2}{3}, \quad \lambda_1 > \frac{3(\omega_1 - \omega_3)(\omega_2 - \omega_1)}{\omega_3 - \omega_2}, \quad (28)$$

$$\omega_2 > -\frac{2}{3}, \quad \lambda_2 > \frac{3(\omega_2 - \omega_1)(\omega_3 - \omega_2)}{\omega_1 - \omega_3}, \quad (29)$$

$$\omega_3 > -\frac{2}{3}, \quad \lambda_3 > \frac{3(\omega_1 - \omega_3)(\omega_3 - \omega_2)}{\omega_2 - \omega_1}. \quad (30)$$

Thus q will be negative when all the $\omega_i > -\frac{2}{3}$. This result corresponds to the quintessence dominated universe.

Note that the vanishing q in Eq. (17) will yield the following state equations

$$q = 0 \implies \omega_1 = \omega_2 = \omega_3 = -\frac{2}{3}. \quad (31)$$

Moreover $q > 0$ corresponds to an decelerating universe. This situation arises in our model when

$$\left(\frac{2}{3} + \omega_1\right)X_1 < 0, \quad (32)$$

$$\left(\frac{2}{3} + \omega_2\right)X_2 < 0, \quad (33)$$

$$\left(\frac{2}{3} + \omega_3\right)X_3 < 0. \quad (34)$$

The above Eqs. (32), (33) and (34) yield respectively

$$\omega_1 < -\frac{2}{3}, \quad \lambda_1 > \frac{3(\omega_1 - \omega_3)(\omega_2 - \omega_1)}{\omega_3 - \omega_2}, \quad (35)$$

$$\omega_2 < -\frac{2}{3}, \quad \lambda_2 > \frac{3(\omega_2 - \omega_1)(\omega_3 - \omega_2)}{\omega_1 - \omega_3}, \quad (36)$$

$$\omega_3 < -\frac{2}{3}, \quad \lambda_3 > \frac{3(\omega_1 - \omega_3)(\omega_3 - \omega_2)}{\omega_2 - \omega_1}. \quad (37)$$

Thus q will be negative when all the $\omega_i < -\frac{2}{3}$. The strength of the interaction is determined by the coupling parameters λ_i . These coupling constants are expressed in terms of the equation of state parameters ω_i . We here stress that the exact nature of the interaction is largely unknown i.e. the mediating particles of the interaction are not yet identified. Any interacting dark energy model should, in principle, be motivated from the particle physics or the corresponding phenomenology, however there are as yet no sound theoretical models which could identify the particle interactions. There are some arguments that the phantom-like dark energy can decay into at least one ordinary particle and some other phantom-like particles [24].

3 Stability analysis

To perform stability analysis, we write Eqs. (2-5) as

$$\dot{\rho}_1 + 3H(1 + \omega_1)\rho_1 = 3H\lambda_1(\rho_3 - \rho_2), \quad (38)$$

$$\dot{\rho}_2 + 3H(1 + \omega_2)\rho_2 = 3H\lambda_2(\rho_1 - \rho_3), \quad (39)$$

$$\dot{\rho}_3 + 3H(1 + \omega_3)\rho_3 = 3H\lambda_3(\rho_2 - \rho_1). \quad (40)$$

Here we have used constraint equations on the coupling parameters by: $\lambda_3 - \lambda_2 = \lambda_1$, $\lambda_1 - \lambda_3 = \lambda_2$ and $\lambda_2 - \lambda_1 = \lambda_3$. Since the above system is autonomous i.e. there is no explicit time dependent term in the equations, we can analyze this system by first finding its critical points and checking its stability about those points. A critical point (also called

fixed point) is the one that satisfies the above system when equated to zero. Similarly, a critical point becomes an attractor point if the solution of the system converges to that point for large values of time parameter.

Further, we define dimensionless parameters as

$$u_1 = \frac{\rho_1}{\rho_{cr}} = \Omega_1, \quad (41)$$

$$u_2 = \frac{\rho_2}{\rho_{cr}} = \Omega_2, \quad (42)$$

$$u_3 = \frac{\rho_3}{\rho_{cr}} = \Omega_3. \quad (43)$$

Using Eqs. (41-43), we can rewrite Eqs (38-40) as

$$\frac{du_1}{dx} = 3u_1\{(1 + \omega_2)u_2 + (1 + \omega_3)u_3\} + 3\lambda_1(u_3 - u_2), \quad (44)$$

$$\frac{du_2}{dx} = 3u_2\{(1 + \omega_1)u_1 + (1 + \omega_3)u_3\} + 3\lambda_2(u_1 - u_3), \quad (45)$$

$$\frac{du_3}{dx} = 3u_3\{(1 + \omega_1)u_1 + (1 + \omega_2)u_2\} + 3\lambda_3(u_2 - u_1). \quad (46)$$

Above the time derivative is replaced with the differentiation with $x = \ln a$. This parameter corresponds to the number of e-foldings which is convenient to use for the dynamics of dark energy. By equating above three equations to zero, we obtain the critical points (see below). To find whether the system approaches to any critical point, we check the stability about these points, by producing small perturbations δu_1 , δu_2 and δu_3 around the critical point (u_{1c}, u_{2c}, u_{3c}) i.e.

$$u_1 = u_{1c} + \delta u_1, \quad u_2 = u_{2c} + \delta u_2, \quad u_3 = u_{3c} + \delta u_3. \quad (47)$$

Now in order to linearize, we take the δ variation of the above equations (44-46) and evaluate them at the critical points $\{(u_{1c_j}, u_{2c_j}, u_{3c_j})\}$, where j is an indexing parameter:

$$\begin{aligned} \frac{d\delta u_1}{dx} = & 3\delta u_1\{(1 + \omega_2)u_{2c_j} + (1 + \omega_3)u_{3c_j}\} + 3\delta u_2\{u_{1c_j}(1 + \omega_2) - \lambda_1\} \\ & + 3\delta u_3\{u_{1c_j}(1 + \omega_3) + \lambda_1\}, \end{aligned} \quad (48)$$

$$\begin{aligned} \frac{d\delta u_2}{dx} = & 3\delta u_2\{(1 + \omega_1)u_{1c_j} + (1 + \omega_3)u_{3c_j}\} + 3\delta u_3\{u_{2c_j}(1 + \omega_3) - \lambda_2\} \\ & + 3\delta u_1\{u_{2c_j}(1 + \omega_1) + \lambda_2\}, \end{aligned} \quad (49)$$

$$\begin{aligned} \frac{d\delta u_3}{dx} = & 3\delta u_3\{(1 + \omega_2)u_{2c_j} + (1 + \omega_1)u_{1c_j}\} + 3\delta u_1\{u_{3c_j}(1 + \omega_1) - \lambda_3\} \\ & + 3\delta u_2\{u_{3c_j}(1 + \omega_2) + \lambda_3\}. \end{aligned} \quad (50)$$

We can easily construct a matrix consisting of the coefficients of the perturbation parameters. Next we can compute the eigenvalues of that matrix. Stability of the critical points

depends on the nature of the eigenvalues. It leads to several cases: if the real parts of all the eigenvalues are negative, then the following critical point is a stable node, if the real parts of the eigenvalues are all positive, then that critical point is an unstable node, in all other cases, the critical points will be saddle points. In our analysis, only those critical points are of interest that yield stable nodes.

In order to obtain some physical interpretation of our results, we designate dust (or matter), radiation and dark energy with subscripts 1, 2 and 3 respectively. Thus the corresponding EoS parameters take values $\omega_1 = 0$, $\omega_2 = 1/3$ and $\omega_3 = -1/3$ or -1 depending whether it is quintessence or cosmological constant. From here we divide our dynamical system (44-46) into two parts: one for $\omega_3 = -1$ and other $\omega_3 = -1/3$.

It is very difficult to obtain the critical points with the above full system (44-46). The only way out is by choosing atleast one λ_i to be zero. In the next sections, we shall use only two coupling parameters while taking the third one to be zero. For instance, taking $\lambda_1 = 0$ implies that radiation and dark energy are mutually non-interacting while there are interactions between dark energy and matter and between matter and radiation. Similar interpretations can be made when choosing either λ_2 or λ_3 to be zero.

3.1 Critical points for $\lambda_1 = 0$

Note that the following critical points are obtained by setting $\lambda_1 = 0$.

3.1.1 Quintessence $\omega_3 = -1/3$

The dynamical system yields the following critical points $\{(u_{1c_j}, u_{2c_j}, u_{3c_j}), j = 1, 2, 3, 4\}$.

$$u_{1c_1} = 0, \quad (51)$$

$$u_{2c_1} = \frac{3}{2}\lambda_2, \quad (52)$$

$$u_{3c_1} = -\frac{3}{4}\lambda_3, \quad (53)$$

$$u_{1c_2} = \frac{1}{48\lambda_2 - 24\lambda_3} \left(-8\lambda_2^2 + \lambda_3 \left(\lambda_3 - \sqrt{16\lambda_2^2 + 568\lambda_2\lambda_3 + \lambda_3^2} \right) - 2\lambda_2 \left(-35\lambda_3 + \sqrt{16\lambda_2^2 + 568\lambda_2\lambda_3 + \lambda_3^2} \right) \right), \quad (54)$$

$$u_{2c_2} = \frac{1}{32} \left(4\lambda_2 - \lambda_3 + \sqrt{16\lambda_2^2 + 568\lambda_2\lambda_3 + \lambda_3^2} \right), \quad (55)$$

$$u_{3c_2} = \frac{1}{16} \left(-4\lambda_2 + \lambda_3 - \sqrt{16\lambda_2^2 + 568\lambda_2\lambda_3 + \lambda_3^2} \right), \quad (56)$$

$$u_{1_{c_3}} = \frac{1}{48\lambda_2 - 24\lambda_3} \left(-8\lambda_2^2 + \lambda_3 \left(\lambda_3 + \sqrt{16\lambda_2^2 + 568\lambda_2\lambda_3 + \lambda_3^2} \right) + 2\lambda_2 \left(-35\lambda_3 + \sqrt{16\lambda_2^2 + 568\lambda_2\lambda_3 + \lambda_3^2} \right) \right), \quad (57)$$

$$u_{2_{c_3}} = \frac{1}{32} \left(4\lambda_2 - \lambda_3 - \sqrt{16\lambda_2^2 + 568\lambda_2\lambda_3 + \lambda_3^2} \right), \quad (58)$$

$$u_{3_{c_3}} = \frac{1}{16} \left(-4\lambda_2 + \lambda_3 + \sqrt{16\lambda_2^2 + 568\lambda_2\lambda_3 + \lambda_3^2} \right), \quad (59)$$

$$u_{4_{c_1}} = 0, \quad (60)$$

$$u_{4_{c_2}} = 0, \quad (61)$$

$$u_{4_{c_3}} = 0. \quad (62)$$

Now we substitute above critical points in Eqs. (38-40) and obtain eigenvalues. Since analytical expressions for the eigenvalues are not possible, so we shall resort to estimate the numerical values of eigenvalues for specific choices of coupling parameters. Fixing $\lambda_2 = 0.5$ and $\lambda_3 = 0.7$ (both positive), $\lambda_2 = 0.5$ and $\lambda_3 = -0.7$ (one positive) and $\lambda_2 = -0.5$ and $\lambda_3 = -0.7$ (both negative) no stable node is obtained from the above critical points. However, for $\lambda_2 = -0.5$ and $\lambda_3 = 0.7$, the first critical point $\{(u_{1_{c_1}}, u_{2_{c_1}}, u_{3_{c_1}})\}$ becomes a stable node.

3.1.2 Cosmological constant $\omega_3 = -1$

$$u_{1_{c_1}} = \lambda_3, \quad (63)$$

$$u_{2_{c_1}} = 0, \quad (64)$$

$$u_{3_{c_1}} = \lambda_3, \quad (65)$$

$$u_{1_{c_2}} = 0, \quad (66)$$

$$u_{2_{c_2}} = 0, \quad (67)$$

$$u_{3_{c_2}} = 0. \quad (68)$$

For all the choices of λ_2 and λ_3 as adopted in the previous subsection, no critical point arises as a stable node.

3.2 Critical points for $\lambda_2 = 0$

Setting $\lambda_2 = 0$, we obtain the following critical points:

3.2.1 Quintessence $\omega_3 = -1/3$

$$u_{1_{c_1}} = -\frac{1}{2}\lambda_1, \quad (69)$$

$$u_{2_{c_1}} = 0, \quad (70)$$

$$u_{3_{c_1}} = \lambda_3, \quad (71)$$

$$u_{1_{c_2}} = \frac{1}{48} \left(-9\lambda_1 - 2\lambda_3 + \sqrt{81\lambda_1^2 + 1476\lambda_1\lambda_3 + 4\lambda_3^2} \right), \quad (72)$$

$$u_{2_{c_2}} = \frac{1}{64(3\lambda_1 - 2\lambda_3)} \left(27\lambda_1^2 - 2\lambda_3 \left(-2\lambda_3 + \sqrt{81\lambda_1^2 + 1476\lambda_1\lambda_3 + 4\lambda_3^2} \right) - 3\lambda_1 \left(72\lambda_3 + \sqrt{81\lambda_1^2 + 1476\lambda_1\lambda_3 + 4\lambda_3^2} \right) \right), \quad (73)$$

$$u_{3_{c_2}} = \frac{1}{32} \left(9\lambda_1 + 2\lambda_3 - \sqrt{81\lambda_1^2 + 1476\lambda_1\lambda_3 + 4\lambda_3^2} \right), \quad (74)$$

$$u_{1_{c_3}} = \frac{1}{48} \left(-9\lambda_1 - 2\lambda_3 - \sqrt{81\lambda_1^2 + 1476\lambda_1\lambda_3 + 4\lambda_3^2} \right), \quad (75)$$

$$u_{2_{c_3}} = \frac{1}{64(3\lambda_1 - 2\lambda_3)} \left(27\lambda_1^2 + 3\lambda_1 \left(-72\lambda_3 + \sqrt{81\lambda_1^2 + 1476\lambda_1\lambda_3 + 4\lambda_3^2} \right) + 2\lambda_3 \left(2\lambda_3 + \sqrt{81\lambda_1^2 + 1476\lambda_1\lambda_3 + 4\lambda_3^2} \right) \right), \quad (76)$$

$$u_{3_{c_3}} = \frac{1}{32} \left(9\lambda_1 + 2\lambda_3 + \sqrt{81\lambda_1^2 + 1476\lambda_1\lambda_3 + 4\lambda_3^2} \right), \quad (77)$$

$$u_{1_{c_4}} = 0, \quad (78)$$

$$u_{2_{c_4}} = 0, \quad (79)$$

$$u_{3_{c_4}} = 0. \quad (80)$$

For $\lambda_1 = 0.5$ and $\lambda_3 = -0.7$, the stable node arises at second critical point $\{(u_{1_{c_2}}, u_{2_{c_2}}, u_{3_{c_2}})\}$. For other values of λ_1 and λ_3 , no other stable node arises.

3.2.2 Cosmological constant $\omega_3 = -1$

$$u_{1_{c_1}} = 0, \quad (81)$$

$$u_{2_{c_1}} = -\frac{3}{4}\lambda_3, \quad (82)$$

$$u_{3_{c_1}} = -\frac{3}{4}\lambda_3, \quad (83)$$

$$u_{1_{c_2}} = 0, \quad (84)$$

$$u_{2_{c_2}} = 0, \quad (85)$$

$$u_{3_{c_2}} = 0. \quad (86)$$

Here for $\lambda_1 = 0.5$ and $\lambda_3 = -0.7$, the stable node arises at second critical point $\{(u_{1_{c_2}}, u_{2_{c_2}}, u_{3_{c_2}})\}$.

3.3 Critical points for $\lambda_3 = 0$

Now we perform similar analysis for $\lambda_3 = 0$, we get the critical points

3.3.1 Quintessence $\omega_3 = -1/3$

$$u_{1c_1} = \frac{3}{4}\lambda_1, \quad (87)$$

$$u_{2c_1} = -\lambda_2, \quad (88)$$

$$u_{3c_1} = 0, \quad (89)$$

$$u_{1c_2} = \frac{1}{48} \left(-9\lambda_1 - 8\lambda_2 + \sqrt{81\lambda_1^2 + 4176\lambda_1\lambda_2 + 64\lambda_2^2} \right), \quad (90)$$

$$u_{2c_2} = \frac{1}{64} \left(9\lambda_1 + 8\lambda_2 - \sqrt{81\lambda_1^2 + 4176\lambda_1\lambda_2 + 64\lambda_2^2} \right), \quad (91)$$

$$u_{3c_2} = \frac{1}{96\lambda_1 - 128\lambda_2} \left(27\lambda_1^2 + 396\lambda_1\lambda_2 + 32\lambda_2^2 - 3\lambda_1 \sqrt{81\lambda_1^2 + 4176\lambda_1\lambda_2 + 64\lambda_2^2} - 4\lambda_2 \sqrt{81\lambda_1^2 + 4176\lambda_1\lambda_2 + 64\lambda_2^2} \right), \quad (92)$$

$$u_{1c_3} = \frac{1}{48} \left(-9\lambda_1 - 8\lambda_2 - \sqrt{81\lambda_1^2 + 4176\lambda_1\lambda_2 + 64\lambda_2^2} \right), \quad (93)$$

$$u_{2c_3} = \frac{1}{64} \left(9\lambda_1 + 8\lambda_2 + \sqrt{81\lambda_1^2 + 4176\lambda_1\lambda_2 + 64\lambda_2^2} \right), \quad (94)$$

$$u_{3c_3} = \frac{1}{96\lambda_1 - 128\lambda_2} \left(27\lambda_1^2 + 396\lambda_1\lambda_2 + 32\lambda_2^2 + 3\lambda_1 \sqrt{81\lambda_1^2 + 4176\lambda_1\lambda_2 + 64\lambda_2^2} + 4\lambda_2 \sqrt{81\lambda_1^2 + 4176\lambda_1\lambda_2 + 64\lambda_2^2} \right), \quad (95)$$

$$u_{1c_4} = 0, \quad (96)$$

$$u_{2c_4} = 0, \quad (97)$$

$$u_{3c_4} = 0. \quad (98)$$

Among the above critical points, the only stable node is produced for the first one for values $\lambda_1 = -0.5$ and $\lambda_2 = 0.7$.

3.3.2 Cosmological constant $\omega_3 = -1$

$$u_{1c_1} = \frac{3}{4}\lambda_1, \quad (99)$$

$$u_{2c_1} = -\lambda_2, \quad (100)$$

$$u_{3c_1} = 0, \quad (101)$$

$$u_{1c_2} = \frac{7\lambda_1\lambda_2}{3\lambda_1 + 4\lambda_2}, \quad (102)$$

$$u_{2c_2} = -\frac{21\lambda_1\lambda_2}{4(3\lambda_1 + 4\lambda_2)}, \quad (103)$$

$$u_{3c_2} = \frac{7\lambda_1\lambda_2(-9\lambda_1 + 16\lambda_2)}{4(3\lambda_1 + 4\lambda_2)^2}, \quad (104)$$

$$u_{1c_3} = 0, \quad (105)$$

$$u_{2c_3} = 0, \quad (106)$$

$$u_{3c_3} = 0. \quad (107)$$

Among the above critical points, the only stable node is produced for the first one for values $\lambda_1 = -0.5$ and $\lambda_2 = 0.7$.

In figures 1-6, we provide the evolution of the Universe controlled by two interacting fluids out of three at a time with varying EoS parameter ω_3 , say $\omega_3 = -1, \omega_3 = \frac{-1}{3}$ with different initial conditions. In figures 1 and 4, we assume first and second interacting fluids whereas in figures 2 and 5 and 3 and 6, we assume second and third and first and third interacting fluids respectively. In figures 7-10, we provide a comparison study of stability for three interacting fluids assuming different coupling parameters. The initial conditions are chosen arbitrarily but these satisfy the constraint $u_1(0) + u_2(0) + u_3(0) = 1$. The graphs indicate initial fluctuation (unstable) and later become flat (stable) and finally asymptotically flat (globally stable).

4 Conclusion and discussion

In this paper, we have attempted to resolve the cosmic triple coincidence problem which naively asks why the energy densities of the three major ingredients of the cosmic composition namely matter, radiation and dark energy are of same order at current time. Rephrasing, why ω has evolved to -1 in recent times. We here point out that the EoS $p = \omega\rho$ used in this paper is not, in general, a true EoS for any cosmic fluid. Rather it is a phenomenological relationship suitable for the configuration. The actual EoS may not be that simple and may have dependencies on various other cosmological parameters like redshift, time, Hubble parameter and its derivatives etc [8]. However to a first order approximation, it may be taken for such analysis. Further, the standard non-interacting FRW model cannot resolve the coincidence problem since it predicts a hierarchical system in which radiation density decreases faster compared to matter, while density of dark energy remains either constant (if it is cosmological constant) or increases (if it is phantom energy). Therefore it contradicts with the observations where all the three components have equivalent densities. Model of interacting dark energy, which is a modification of

the FRW model, has enormous potential to explain this cosmological conundrum. It naturally predicts that if the cosmic fluids interact with each other, it leads to a scenario compatible with the observations [23].

We have found that in the interacting fluid model, the three fluids can achieve super-negative equation of state. If matter and radiation are among the components then they will induce negative pressure along with the dark energy to produce accelerated expansion. This result has earlier been shown for the interacting Chaplygin gas model in [7]. Moreover the three components can induce deceleration and de Sitter expansion by interacting cohesively.

Acknowledgments

One of us (MJ) would like to thank John D. Barrow for useful correspondence. Useful comments from the anonymous referee are also gratefully acknowledged.

References

- [1] P.J. Steinhardt et al, Phys. Rev. Lett. 59 (1999) 123504.
- [2] L. Wang et al, Phys. Rev. Lett. 82 (1999) 896.
- [3] S. Nojiri et al, arXiv: hep-th/0603062.
- [4] F. Rahaman et al, arXiv: gr-qc/0809.4314v1 .
- [5] N. Arkani-Hamed et al, Phys. Rev. Lett. 85 (2000) 4434.
- [6] H. Stefancic, arXiv: astro-ph/0504518v3.
- [7] M. Jamil and M.A. Rashid, Eur. Phys. J. C 58 (2008) 111.
- [8] M. Jamil and M.A. Rashid, Eur. Phys. J. C 56 (2008) 249.
- [9] M. Jamil and M.A. Rashid, Eur. Phys. J. C 60 (2009) 141
- [10] M. Szydlowski, Phys. Lett. B 632 (2006) 1.
- [11] J.D. Barrow and T. Clifton, Phys. Rev. D 73 (2006) 103520
- [12] A. de la Macorra, arXiv: astro-ph/0701635v1
- [13] N.P. Neto and B.M.O. Fraga, Gen. Relativ. Gravit. 40 (2008) 1653.
- [14] M.R. Setare, Eur. Phys. J. C 52 (2007) 689.
- [15] M. Jamil, arXiv: gr-qc/0810.2896v2
- [16] S. Nojiri and S.D. Odintsov, arXiv: hep-th/0505215
- [17] W. Zimdahl and D. Pavon, Gen. Relativ. Gravit. 36 (2004) 1483.
- [18] L.P. Cimento et al, Phys. Rev. D 67 (2003) 087302.
- [19] N. Cruz et al, Phys. Lett. B 663 (2008) 338.
- [20] H.M. Sadjadi and M. Alimohammadi, Phys. Rev. D 74 (2006) 103007.
- [21] H. Wei and S.N. Zhang, Phys. Lett. B 654 (2007) 139.
- [22] C. Feng et al, Phys. Lett. B 665 (2008) 111.
- [23] S. del Campo et al, Phys. Rev. D 74 (2006) 023501.
- [24] S. Carroll et al, Phys. Rev. D 68 (2003) 023509.
- [25] I. Brevik et al, Eur. Phys. J. C 52 (2007) 223

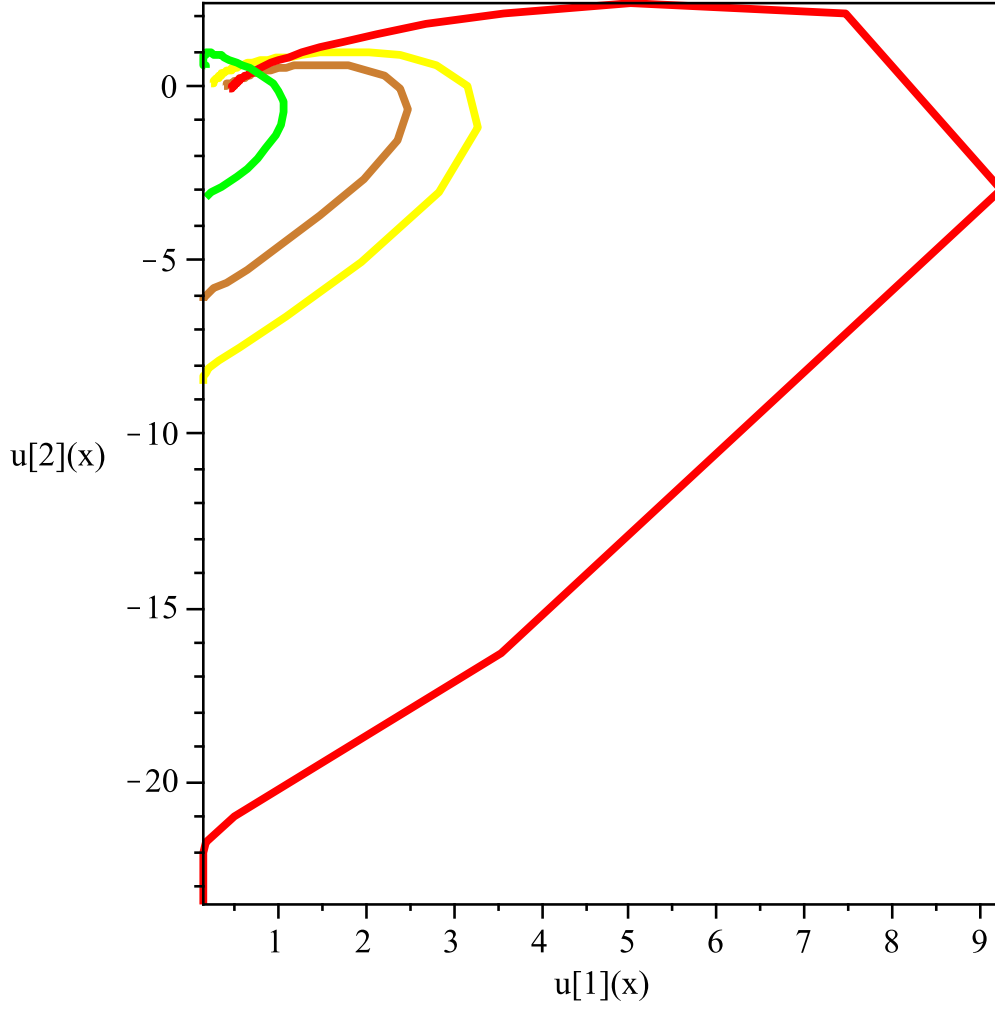


Figure 1: The phase diagram of the triple interacting fluid model with the choice of couplings $[\lambda_1 = 0.2, \lambda_2 = 0.8, \lambda_3 = 0.4]$, $x = -0.8, \dots, 0.8$ and EoS parameters $[\omega_1 = 0, \omega_2 = 1/3, \omega_3 = -1]$. Chosen scene is between u_1 and u_2 . The curved lines correspond to the initial conditions $u_1(0) = 0.8, u_2(0) = 0.4, u_3(0) = 0.8$ (brown); $u_1(0) = 0.6, u_2(0) = 0.6, u_3(0) = 0.6$ (yellow); $u_1(0) = 0.7, u_2(0) = 0.4, u_3(0) = 0.4$ (red); $u_1(0) = 0.3, u_2(0) = 0.9, u_3(0) = 1$ (green).

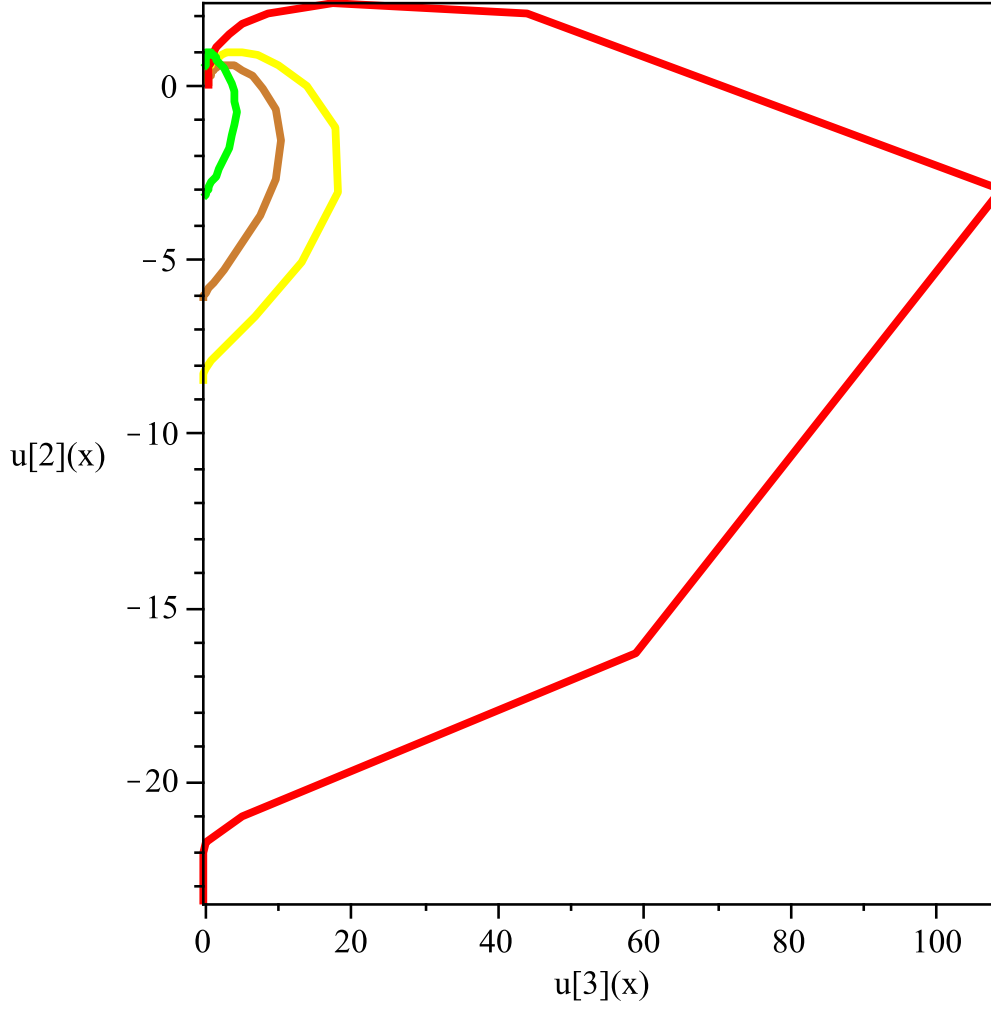


Figure 2: The phase diagram of the triple interacting fluid model with the choice of couplings $[\lambda_1 = 0.2, \lambda_2 = 0.8, \lambda_3 = 0.4]$, $x = -0.8, \dots, 0.8$ and EoS parameters $[\omega_1 = 0, \omega_2 = 1/3, \omega_3 = -1]$. Chosen scene is between u_2 and u_3 . The curved lines correspond to the initial conditions $u_1(0) = 0.8, u_2(0) = 0.4, u_3(0) = 0.8$ (brown); $u_1(0) = 0.6, u_2(0) = 0.6, u_3(0) = 0.6$ (yellow); $u_1(0) = 0.7, u_2(0) = 0.4, u_3(0) = 0.4$ (red); $u_1(0) = 0.3, u_2(0) = 0.9, u_3(0) = 1$ (green).

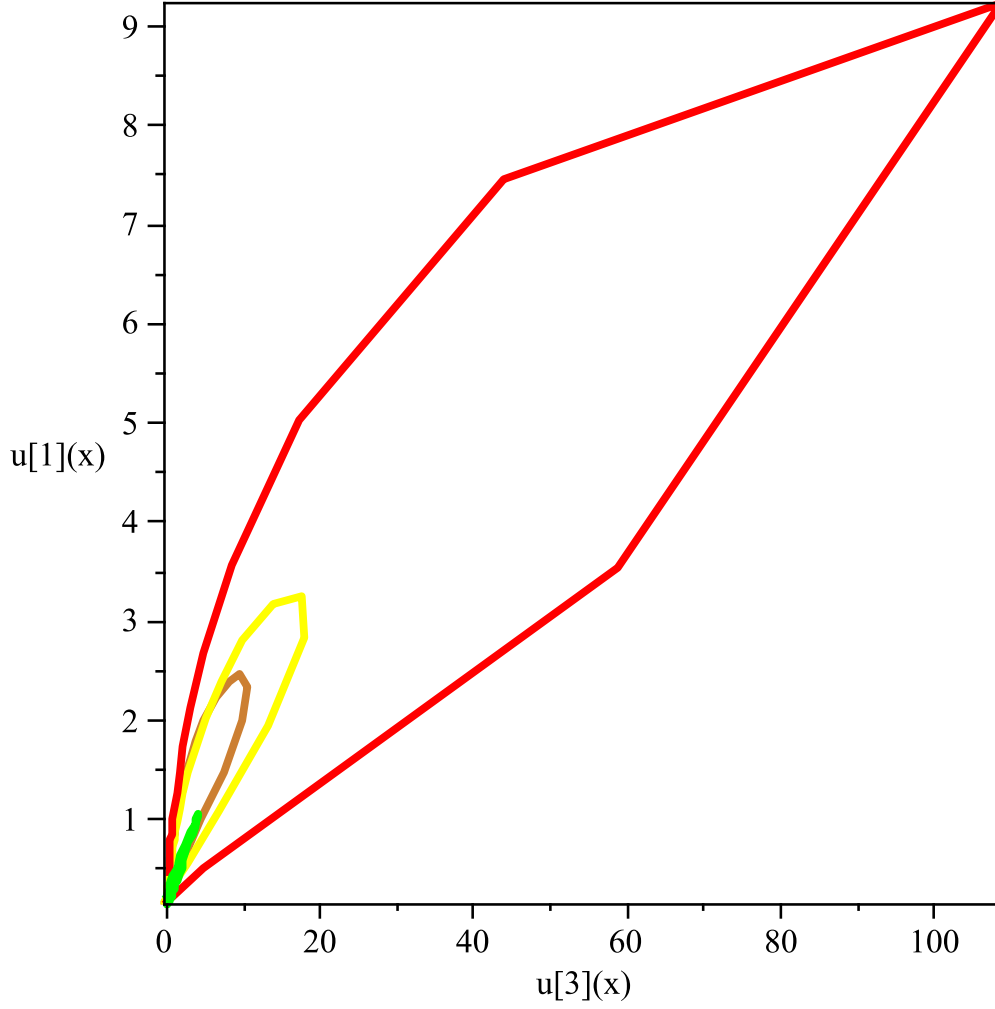


Figure 3: The phase diagram of the triple interacting fluid model with the choice of couplings $[\lambda_1 = 0.2, \lambda_2 = 0.8, \lambda_3 = 0.4]$, $x = -0.8, \dots, 0.8$ and EoS parameters $[\omega_1 = 0, \omega_2 = 1/3, \omega_3 = -1]$. Chosen scene is between u_1 and u_3 . The curved lines correspond to the initial conditions $u_1(0) = 0.8, u_2(0) = 0.4, u_3(0) = 0.8$ (brown); $u_1(0) = 0.6, u_2(0) = 0.6, u_3(0) = 0.6$ (yellow); $u_1(0) = 0.7, u_2(0) = 0.4, u_3(0) = 0.4$ (red); $u_1(0) = 0.3, u_2(0) = 0.9, u_3(0) = 1$ (green).

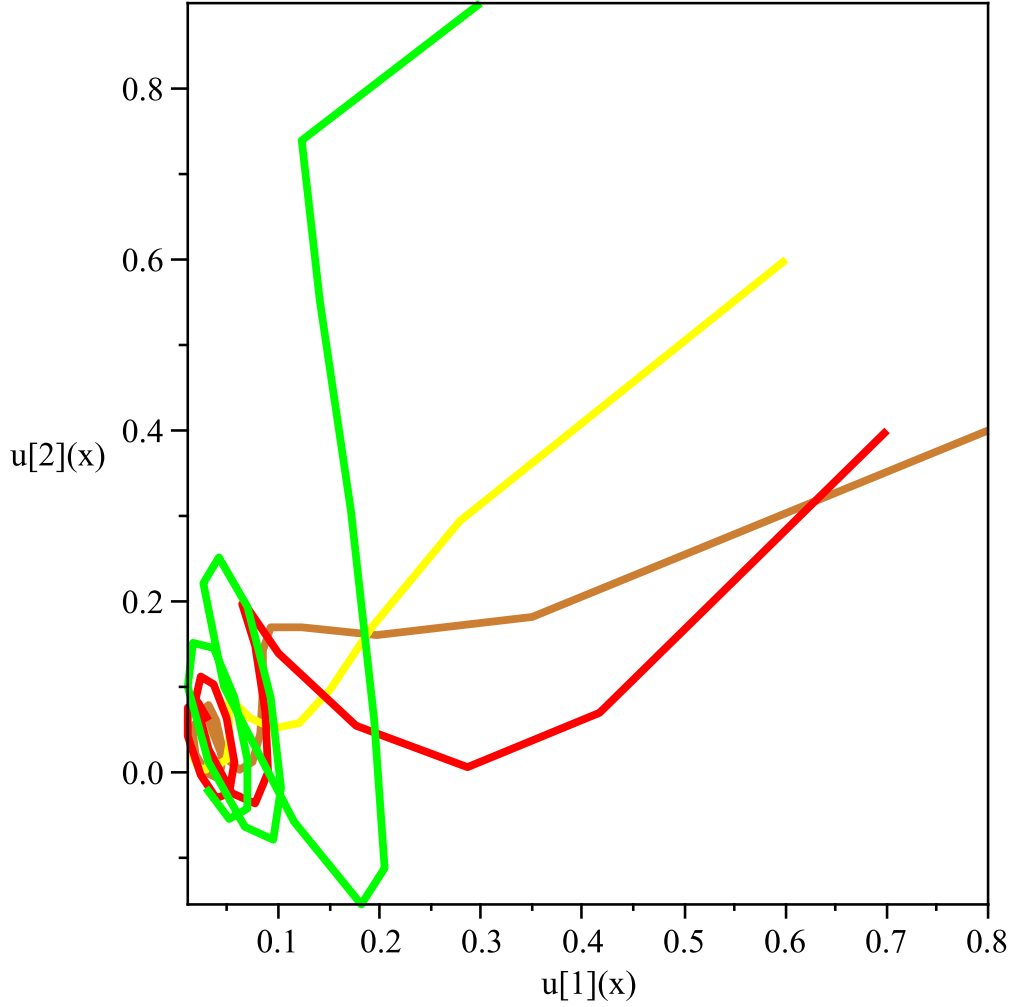


Figure 4: The phase diagram of the triple interacting fluid model with the choice of couplings $[\lambda_1 = 0.2, \lambda_2 = 0.8, \lambda_3 = 0.4]$, $x = -8, \dots, 8$ and EoS parameters $[\omega_1 = 0, \omega_2 = 1/3, \omega_3 = -1/3]$. Chosen scene is between u_1 and u_2 . The curved lines correspond to the initial conditions $u_1(0) = 0.8, u_2(0) = 0.4, u_3(0) = 0.8$ (brown); $u_1(0) = 0.6, u_2(0) = 0.6, u_3(0) = 0.6$ (yellow); $u_1(0) = 0.7, u_2(0) = 0.4, u_3(0) = 0.4$ (red); $u_1(0) = 0.3, u_2(0) = 0.9, u_3(0) = 1$ (green).

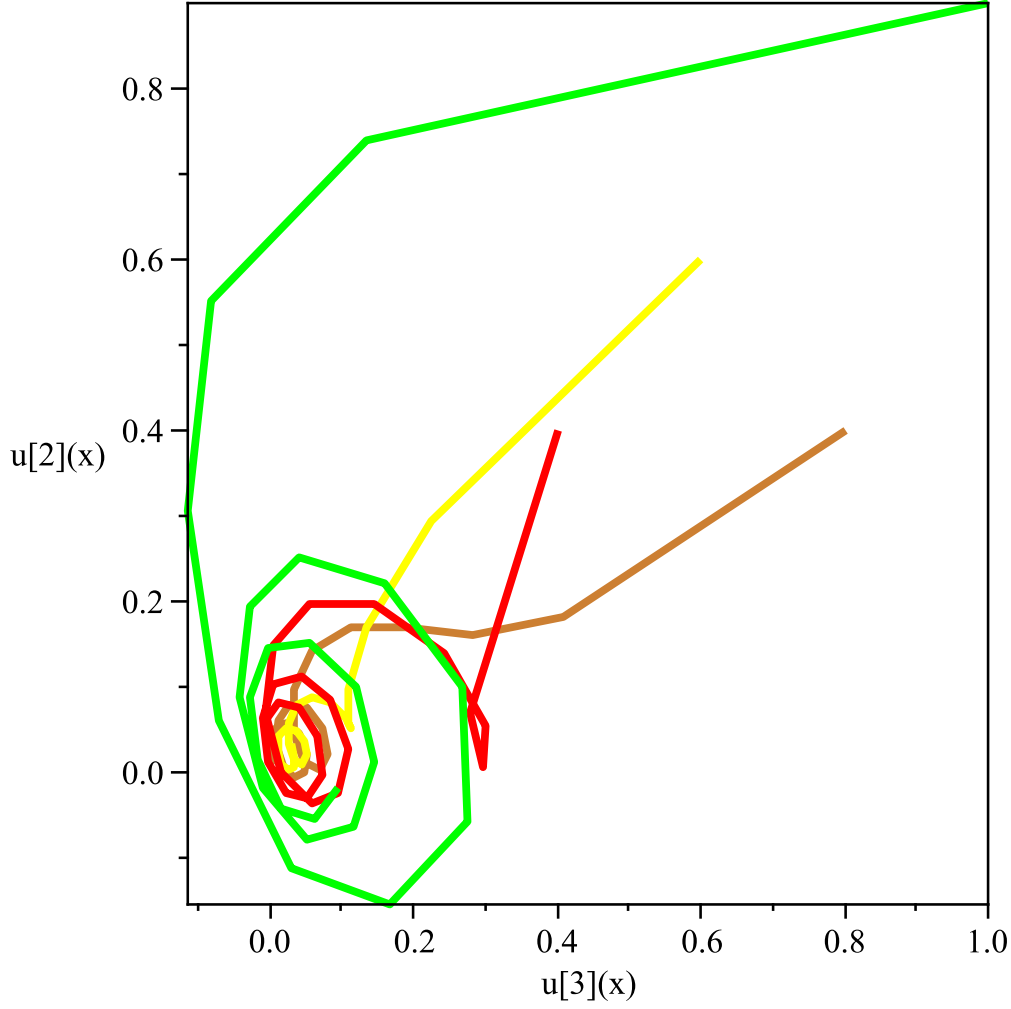


Figure 5: The phase diagram of the triple interacting fluid model with the choice of couplings $[\lambda_1 = 0.2, \lambda_2 = 0.8, \lambda_3 = 0.4]$, $x = -8, \dots, 8$ and EoS parameters $[\omega_1 = 0, \omega_2 = 1/3, \omega_3 = -1/3]$. Chosen scene is between u_2 and u_3 . The curved lines correspond to the initial conditions $u_1(0) = 0.8, u_2(0) = 0.4, u_3(0) = 0.8$ (brown); $u_1(0) = 0.6, u_2(0) = 0.6, u_3(0) = 0.6$ (yellow); $u_1(0) = 0.7, u_2(0) = 0.4, u_3(0) = 0.4$ (red); $u_1(0) = 0.3, u_2(0) = 0.9, u_3(0) = 1$ (green).

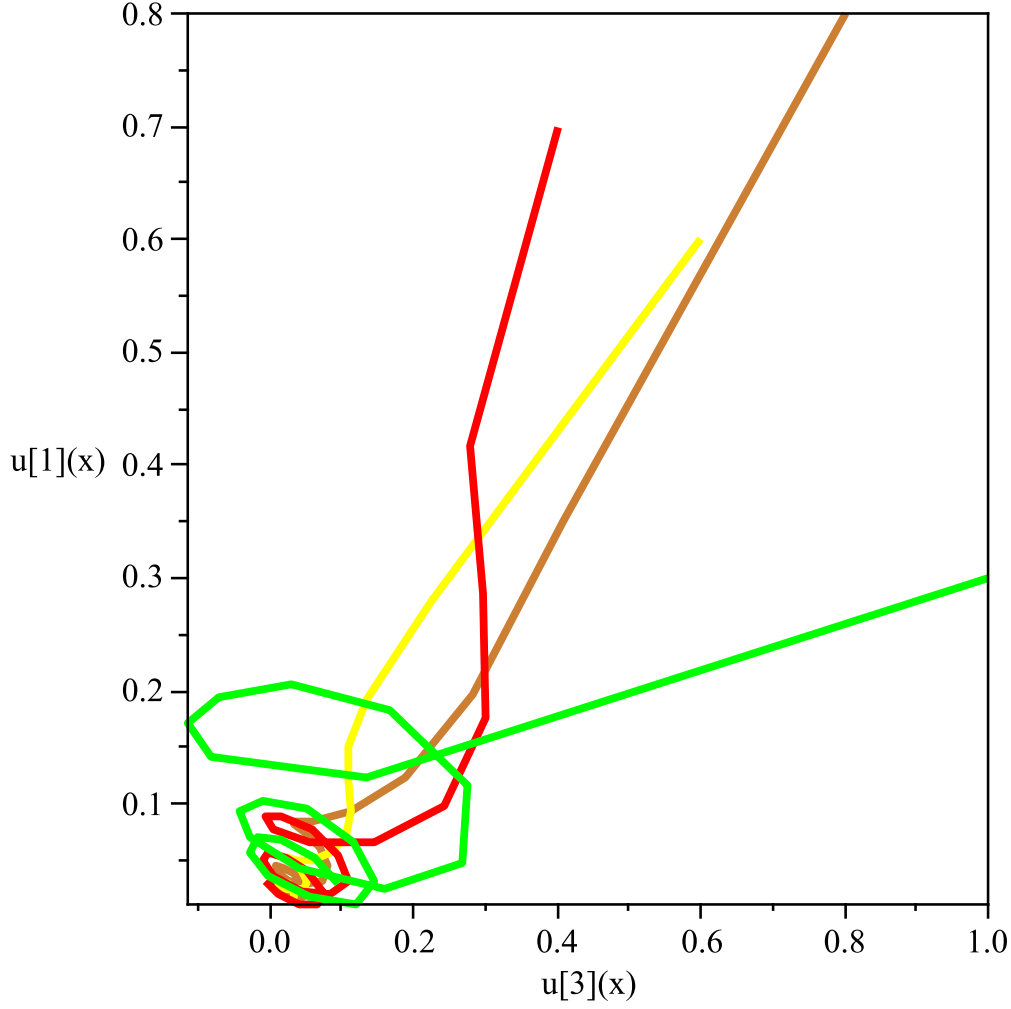


Figure 6: The phase diagram of the triple interacting fluid model with the choice of couplings $[\lambda_1 = 0.2, \lambda_2 = 0.8, \lambda_3 = 0.4]$, $x = -8, \dots, 8$ and EoS parameters $[\omega_1 = 0, \omega_2 = 1/3, \omega_3 = -1/3]$. Chosen scene is between u_1 and u_3 . The curved lines correspond to the initial conditions $u_1(0) = 0.8, u_2(0) = 0.4, u_3(0) = 0.8$ (brown); $u_1(0) = 0.6, u_2(0) = 0.6, u_3(0) = 0.6$ (yellow); $u_1(0) = 0.7, u_2(0) = 0.4, u_3(0) = 0.4$ (red); $u_1(0) = 0.3, u_2(0) = 0.9, u_3(0) = 1$ (green).

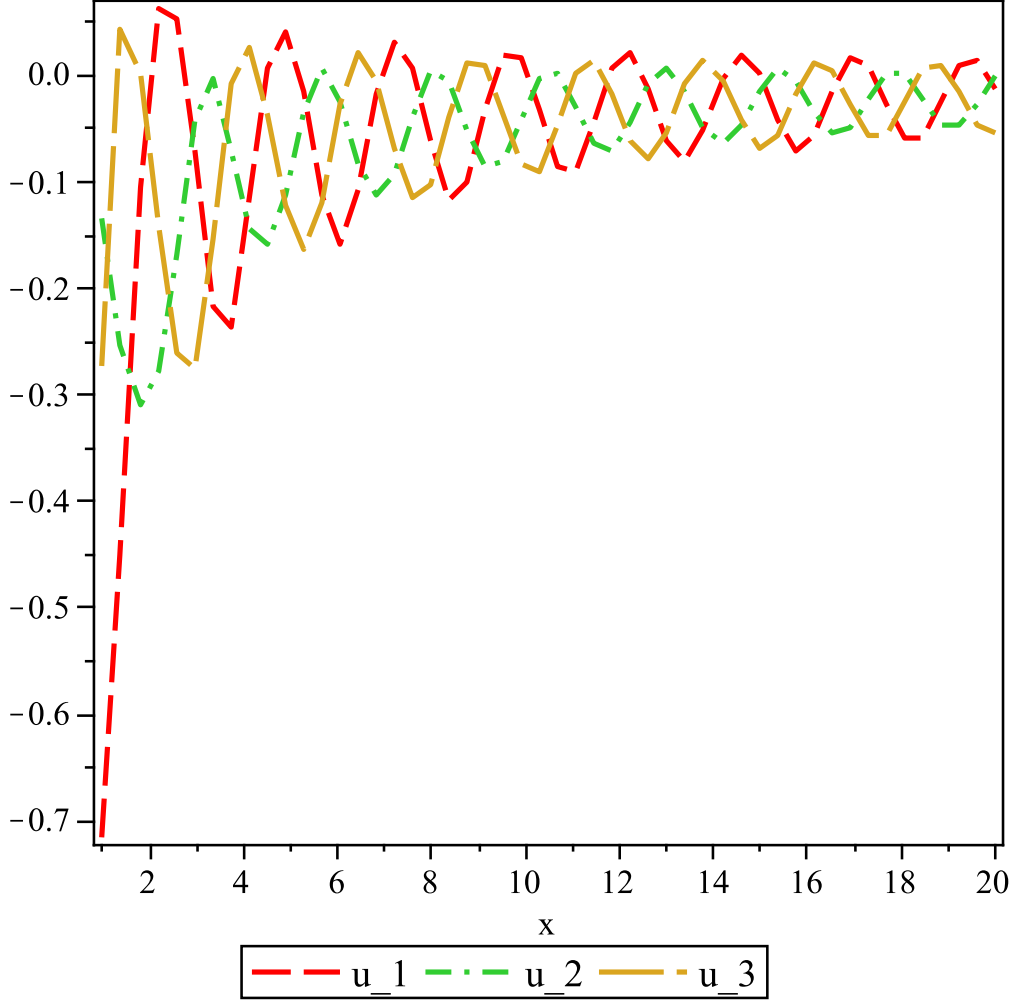


Figure 7: The parametric functions $u_1(x)$, $u_2(x)$ and $u_3(x)$ are plotted against the e-folding time parameter x . The coupling parameters are fixed at $\lambda_1 = -0.6$, $\lambda_2 = 0.4$ and $\lambda_3 = 0.5$ while EoS parameters are $\omega_1 = 0$, $\omega_2 = 1/3$ and $\omega_3 = -1$. The initial conditions are $u_1(0) = 4$, $u_2(0) = -1$, $u_3(0) = -2$.

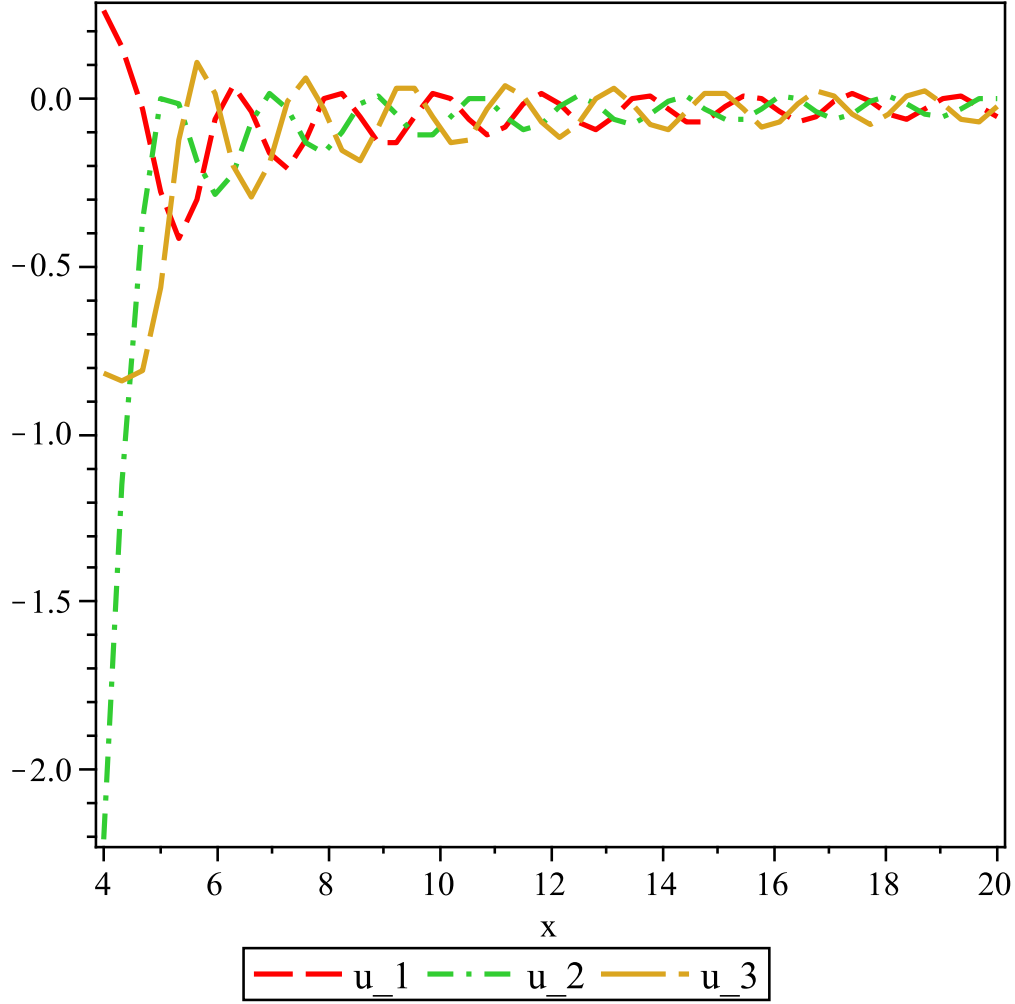


Figure 8: The parametric functions $u_1(x)$, $u_2(x)$ and $u_3(x)$ are plotted against the e-folding time parameter x . The coupling parameters are fixed at $\lambda_1 = 0.6$, $\lambda_2 = 0.5$ and $\lambda_3 = 0.9$ while EoS parameters are $\omega_1 = 0$, $\omega_2 = 1/3$ and $\omega_3 = -1/3$. The initial conditions are $u_1(0) = 5$, $u_2(0) = -10$, $u_3(0) = 6$.

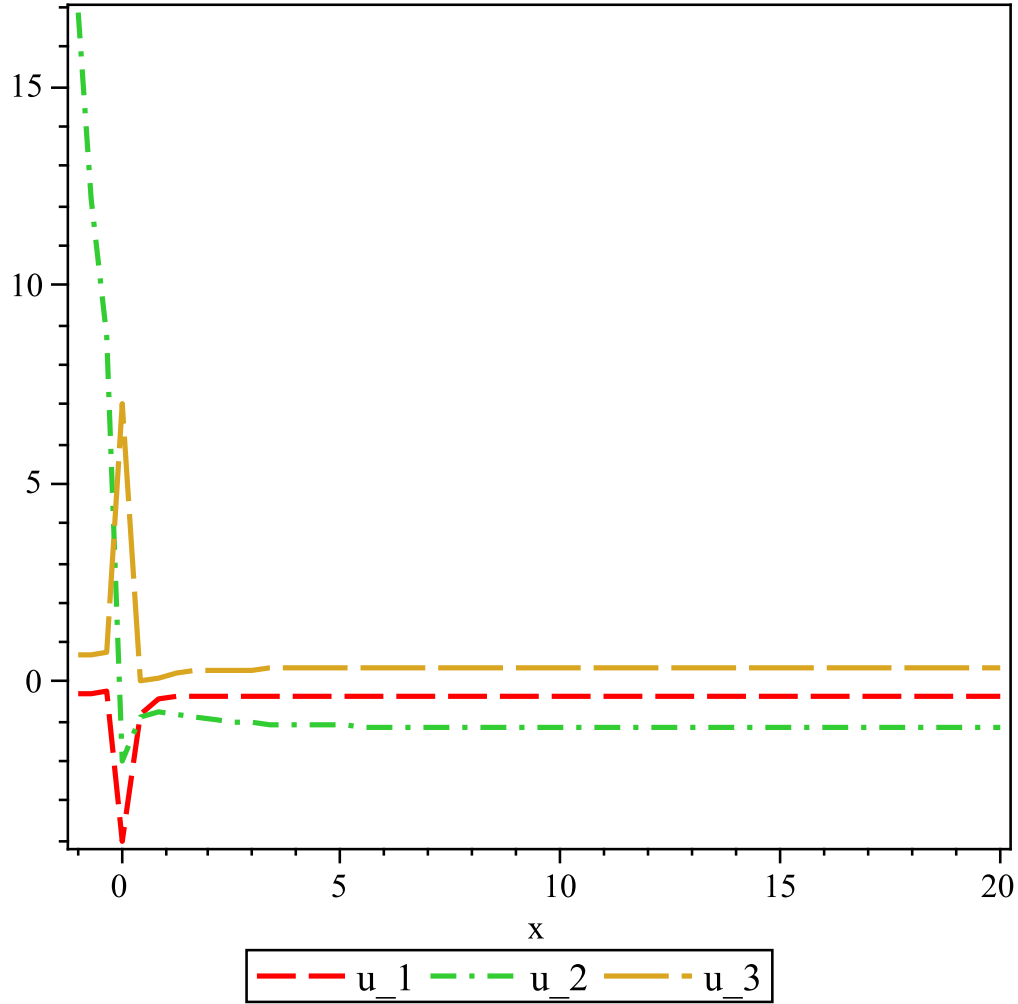


Figure 9: The parametric functions $u_1(x)$, $u_2(x)$ and $u_3(x)$ are plotted against the e-folding time parameter x . The coupling parameters are fixed at $\lambda_1 = -0.4$, $\lambda_2 = 0.6$ and $\lambda_3 = -0.9$ while EoS parameters are $\omega_1 = 0$, $\omega_2 = 1/3$ and $\omega_3 = -1$. The initial conditions are $u_1(0) = -4$, $u_2(0) = -2$, $u_3(0) = 7$.

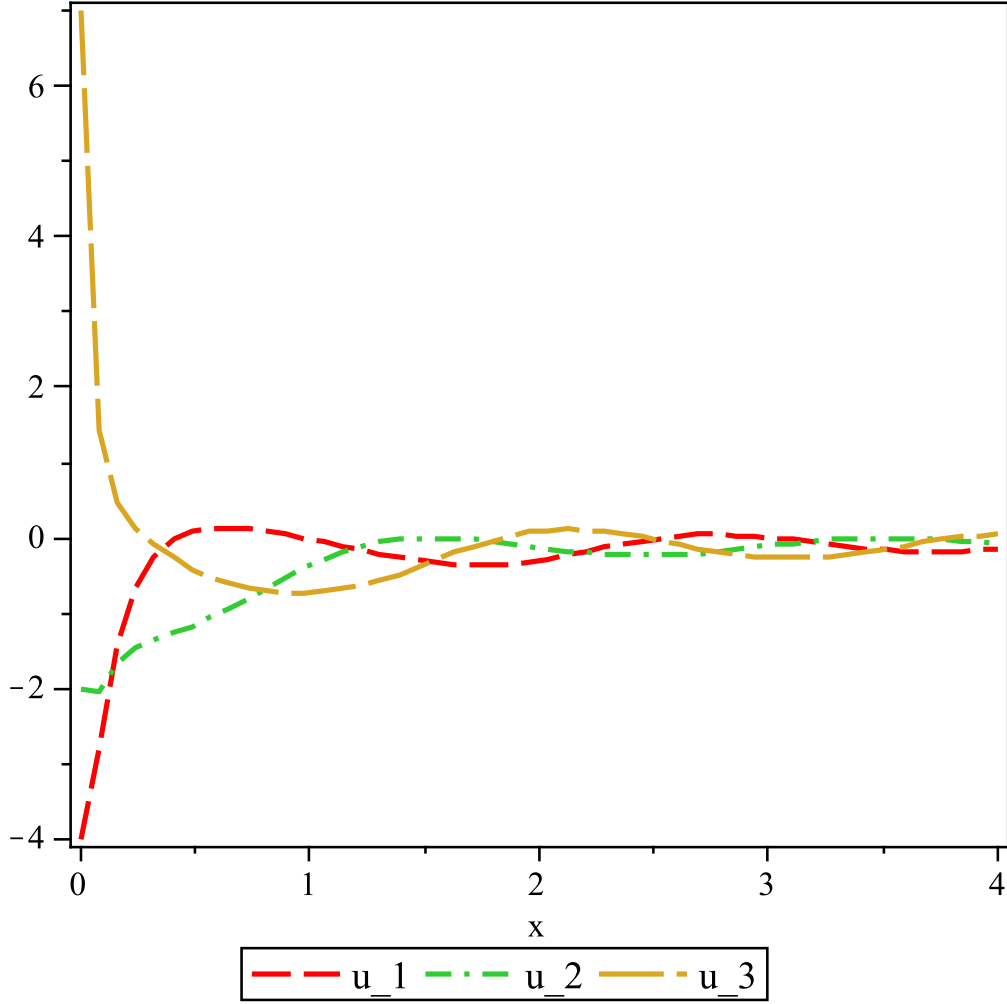


Figure 10: The parametric functions $u_1(x)$, $u_2(x)$ and $u_3(x)$ are plotted against the e-folding time parameter x . The coupling parameters are fixed at $\lambda_1 = 0.6$, $\lambda_2 = 0.4$ and $\lambda_3 = 0.9$ while EoS parameters are $\omega_1 = 0$, $\omega_2 = 1/3$ and $\omega_3 = -1/3$. The initial conditions are $u_1(0) = -4$, $u_2(0) = -2$, $u_3(0) = 7$.